Human dendritic cells (DCs) are derived from distinct circulating precursors that are precommitted to become CD1c$^+$ or CD141$^+$ DCs

Gaëlle Breton,[1] Shiwei Zheng,[2,5] Renan Valieris,[4] Israel Tojal da Silva,[4] Rahul Satija,[2,5] and Michel C. Nussenzweig[1,3]

[1]Laboratory of Molecular Immunology, The Rockefeller University, New York, NY 10065
[2]New York Genome Center, New York, NY 10013
[3]Howard Hughes Medical Institute, Chevy Chase, MD 20815
[4]Laboratory of Computational Biology and Bioinformatics, Centro Internacional de Pesquisa, A.C. Camargo Cancer Center, São Paulo 01509-010, Brazil
[5]Center for Genomics and Systems Biology, New York University, New York, NY 10012

In humans, conventional dendritic cells (cDCs) exist as two unique populations characterized by expression of CD1c and CD141. cDCs arise from increasingly restricted but well-defined bone marrow progenitors that include the common DC progenitor that differentiates into the pre-cDC, which is the direct precursor of cDCs. In this study, we show that pre-cDCs in humans are heterogeneous, consisting of two distinct populations of precursors that are precommitted to become either CD1c$^+$ or CD141$^+$ cDCs. The two groups of lineage-primed precursors can be distinguished based on differential expression of CD172a. Both subpopulations of pre-cDCs arise in the adult bone marrow and can be found in cord blood and adult peripheral blood. Gene expression analysis revealed that CD172a$^+$ and CD172a$^-$ pre-cDCs represent developmentally discrete populations that differentially express lineage-restricted transcription factors. A clinical trial of Flt3L injection revealed that this cytokine increases the number of both CD172a$^-$ and CD172a$^+$ pre-cDCs in human peripheral blood.

INTRODUCTION

DCs are specialized antigen-presenting cells that initiate T cell–mediated immune responses and function as key mediators of immunity and tolerance (Steinman and Hemmi, 2006; Steinman and Banchereau, 2007; Manicassamy and Pulendran, 2011). This cell type can be subdivided into subsets with different origins, anatomical location, and immunological function.

There are three major subsets of DCs in humans. Plasmacytoid DCs (pDCs) are specialized to produce type I IFN and can be identified by expression of BDCA-2/CD303 (Colonna et al., 2004). The other two subsets are conventional DCs (cDCs) that can be distinguished in part by expression of BDCA-1 and BDCA-3, CD1c$^+$, and CD141$^+$ cDCs, respectively. CD1c$^+$ cDCs excel in CD4$^+$ T cell priming (Cohn et al., 2013; Jin et al., 2014) and promote Th17- and Th2-biased immune responses to extracellular pathogens (Persson et al., 2013; Schlitzer et al., 2013). In contrast, CD141$^+$ cDCs are thought to induce Th1 responses and specialize in cross-presentation and CD8$^+$ T cell priming for tumors and pathogens that do not directly infect DCs (Robbins et al., 2008; Bachem et al., 2010; Crozat et al., 2010; Jongbloed et al., 2010; Poulin et al., 2010; Villadangos and Shortman, 2010).

All three of these DC subsets originate from a common progenitor, the human monocyte and DC progenitor that gives rise to monocytes and a common DC progenitor (Lee et al., 2015). Common DC progenitors are restricted to the bone marrow where they give rise to pDCs and a circulating cDC precursor (pre-cDC) that produces the two major subsets of cDCs found in peripheral lymphoid organs (Breton et al., 2015b).

Although pre-cDCs have the potential to differentiate into CD1c$^+$ and CD141$^+$ cDCs, clonal analysis revealed that most pre-cDCs appear to be committed to differentiating into either one or the other subset (Breton et al., 2015b). Consistent with this observation two recent studies showed that the mouse pre-cDCs consist of two precommitted subpopulations of cells that can be distinguished based on differential expression of Siglec-H/Ly6C (Schlitzer et al., 2015) or CD117/CD115 (Grajales-Reyes et al., 2015).

To determine whether there are two distinct precursor populations of differentially regulated cDCs in humans that are committed to either the CD1c$^+$ or CD141$^+$ cDC fate, we examine the transcriptomic signatures of single pre-cDCs and their response to Flt3L infusion in volunteers.

Correspondence to Gaëlle Breton: gbreton@rockefeller.edu

Abbreviations used: cDC, conventional DC; PC, principal component; pDC, plasmacytoid DC; pre-cDC, cDC precursor; SCF, stem cell factor.

The Rockefeller University Press $30.00
J. Exp. Med. 2016 Vol. 213 No. 13 2861–2870
https://doi.org/10.1084/jem.20161135

RESULTS AND DISCUSSION

Human pre-cDCs are heterogeneous

To document potential heterogeneous gene expression by human cDCs and pre-cDCs, we isolated single CD1c$^+$ and CD141$^+$ cDCs from blood and pre-cDCs from cord blood and performed single-cell mRNA sequencing (Fig. 1, a–d). CD1c$^+$ cDCs and CD141$^+$ cDCs represent two separate and transcriptionally distinct groups of cells that were homogeneous for known markers. CD1c$^+$ cDCs selectively express Clec10A, CD1c, ZEB2, and ETS2, whereas the CD141$^+$ cDCs selectively express Clec9A, IDO1, and IRF8 (Fig. 1 b and Table S1).

In contrast, single-cell mRNA sequencing revealed transcriptional heterogeneity within cord blood pre-cDCs. Unsupervised clustering identified three clusters of different cells within this group (Fig. 1 d and Table S2). A small percentage of pre-cDCs expresses cell-surface markers and transcription factors associated with CD141$^+$ cDCs ($P < 1e-27$; Fisher's exact test), such as Clec9A, IDO1, IRF8, BATF3, HLA-DR, CD135/Flt3, and CD117/cKit (CD141$^+$ lineage–primed pre-cDCs; Fig. 1 e). A second larger group of pre-cDCs expresses genes associated with the CD1c$^+$ cDC fate ($P < 1e-28$; Fisher's exact test), such as Clec10A, CD1c, IRF4, HLA-DR, CD11c, and IRF8 (CD1c$^+$ lineage–primed pre-cDCs; Fig. 1 e). The third group of cells does not express genes associated with cDC differentiation ($P > 0.1$; Fisher's exact test) and instead is characterized by CSF-R, CD172a, CD11c, and IRF8 expression (non-DCs; Fig. 1 e). These cells could represent a monocyte precursor contaminating our pre-cDC population; indeed CD115 is a very weak marker, which could explain why we get contamination by monocyte precursors when sorting CD115$^-$ pre-cDCs. In conclusion, human pre-cDCs are a heterogeneous group of cells that contain progenitors that appear to be precommitted to the CD141$^+$ or CD1$^+$ cDC fate.

Human pre-cDCs can be subdivided by CD172a expression

Within cDCs, CD172a/SIRPα is selectively expressed by human CD1c$^+$ cDCs and by mouse CD4$^+$ DCs, which represent their functional equivalent (Fig. 2 a). Moreover, this marker is also expressed by the circulating precursor of mouse CD4$^+$ DCs, the pre–CD4 DC (Grajales-Reyes et al., 2015). Using flow cytometry, we determined whether CD172a expression is heterogeneous in adult human bone marrow, cord blood, and peripheral blood pre-cDCs (Fig. 2 b). Pre-cDCs can be separated into CD172a$^-$, CD172a^{intermediate} (CD172a^{int}), and CD172a$^+$ cells in all cell sources examined, but the relative proportion of the three varies. Bone marrow and cord blood contain a higher frequency of CD172a^{int} pre-cDCs than CD172a$^-$ and CD172a$^+$ pre-cDCs. However, most adult volunteers showed greater numbers of CD172a$^+$ than CD172a$^-$ and CD172a^{int} pre-cDCs in circulation (Fig. 2 b).

To further characterize the cord blood pre-cDC subpopulations, we measured gene expression on CD172a$^-$ and CD172a$^+$ subsets purified by cell sorting. By sparse hierarchical clustering, CD172a$^-$ and CD172a$^+$ pre-cDCs are developmentally distinct from each other and from the mature cDC subsets (Fig. 2 c and Table S3). Moreover, CD172a$^-$ pre-cDCs cluster with CD141$^+$ cDCs and CD172a$^+$ pre-cDCs with CD1c$^+$ cDCs. This observation is consistent with the higher expression of IRF8, BATF3, and ID2 by the CD172a$^-$ pre-cDCs and ETS2, ZEB2, and IRF4 by CD172a$^+$ pre-cDCs. SPI1, which is required for the development of all DCs, is expressed by both subsets of pre-cDCs (Fig. 2 d). Together, the data suggest that the CD172a$^-$ and CD172a$^+$ pre-cDCs represent precommitted cDC progenitors.

To determine whether differential expression of CD172a can be used to identify cells committed to the CD141$^+$ or CD1c$^+$ cDC fate, we fractionated cord blood pre-cDCs on the basis of CD172a expression and cultured them in vitro in the presence of MS-5 stromal cells, Flt3L, stem cell factor (SCF), and GM-CSF (MS5 + FSG; Fig. 2 f; Breton et al., 2015a). Under these conditions, CD172a$^-$ pre-cDCs primarily produce CD141$^+$ cDCs, whereas the CD172a$^+$ pre-cDCs predominantly give rise to CD1c$^+$ cDCs. Of note, culture-derived CD1c$^+$ cDCs are known to acquire CD14 expression in culture (Lee et al., 2015). The CD172a^{int} fraction gives rise to both cDC subsets (Fig. 2, e and g). However, in clonal assays, we were unable to identify cells with the potential to give rise to both CD1c$^+$ and CD141$^+$ cDC subsets, suggesting that the CD172a^{int} population represents a mixture of CD141$^+$ and CD1c$^+$ precommitted cells (Fig. 2 h). Importantly, we did not find uncommitted cells in pre-cDCs (CD34$^-$ cells), but we cannot exclude that these cells exist in the CD34$^+$ hematopoietic stem and progenitor cells. Both pre-cDC subsets can proliferate, but CD141$^+$-committed pre-cDCs have undergone at least one to two more divisions than CD1c$^+$-committed pre-DCs, suggesting that these cells, which have a greater proliferative capacity, are less mature than CD1c$^+$-committed pre-cDCs (Fig. 2 i).

In conclusion, human pre-cDCs are a mixture of cells committed to either the CD141$^+$ lineage (CD172a$^-$ pre-cDCs) or the CD1c$^+$ lineage (CD172a$^+$ pre-cDCs). Our observations are consistent with recent work showing that myeloid progenitors in humans are heterogeneous mixtures of progenitors that are precommitted to a specific lineage (Paul et al., 2015; Perié et al., 2015; Notta et al., 2016).

Peripheral blood pre-cDCs

In addition to cord blood, pre-cDCs can also be isolated from the peripheral blood (Breton et al., 2015b). Single-cell mRNA sequencing of pre-cDCs isolated from peripheral blood showed a pattern of gene expression similar to cord blood pre-cDCs. Unsupervised clustering showed three distinct populations of circulating pre-cDCs: CD141$^+$ lineage–primed cells ($P < 1e-23$; Fisher's exact test), CD1c$^+$ lineage–primed cells ($P < 1e-14$; Fisher's exact test), and non-DCs (Fig. 3 a and Table S4; $P > 0.1$; Fisher's exact test). The majority of the cells were CD1c$^+$ lineage primed and expressed CD172a, which is expected because the majority of peripheral blood pre-cDCs are CD172a$^+$ cells (Fig. 2 b, and Fig 3, a and b).

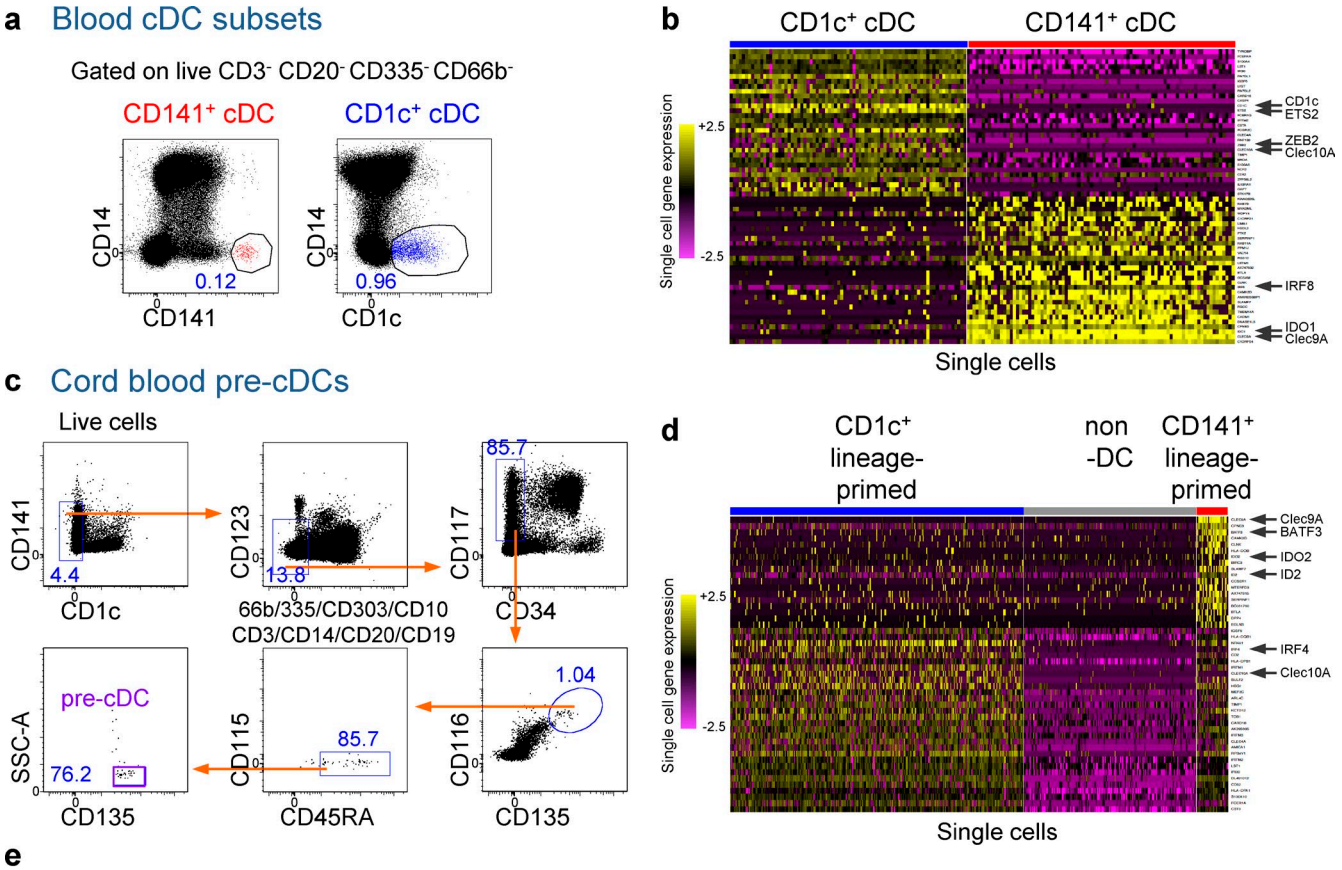

Figure 1. **Heterogeneity in human pre-cDCs revealed by single-cell mRNA sequencing.** (a) Gating strategy for isolation of CD1c$^+$ cDCs and CD141$^+$ cDCs in blood. CD1c$^+$ cDCs (blue) and CD141$^+$ cDCs (red) are identified in live CD3$^-$ CD20$^-$ CD335$^-$ CD66b$^-$ cells, i.e., T, B, NK, and neutrophil cell depleted based on the expression of CD1c and CD141, respectively, and the absence of CD14 expression ($n = 5$). Gate frequencies from the parent population are shown. (b) Unsupervised clustering reveals transcriptomic signatures of single differentiated blood cDCs, i.e., CD1c$^+$ cDCs (77 single cells; blue) and CD141$^+$ cDCs (87 single cells; red; three samples). Shown are the top 30 genes exhibiting the strongest differential expression for each subset ($P < 10^{-5}$; likelihood ratio test for single-cell differential expression; see the Single-cell mRNA sequencing section of Materials and methods and Table S1). (c) Gating strategy for isolation of human pre-cDCs in cord blood. Live CD3$^-$ CD20$^-$ CD19$^-$ CD335$^-$ CD66b$^-$ CD14$^-$ CD1c$^-$ CD141$^-$ CD303$^-$ cells, i.e., T cell, B cell, NK cell, neutrophil, monocyte, and DC depleted, were stained for CD34, CD117, CD123, CD135, CD116, CD115, and CD45RA markers. CD34$^-$ CD117$^+$ CD123$^{-/+}$ CD135$^+$ CD116$^+$ CD115$^-$ CD45RA$^+$ pre-cDCs are shown. Gate frequencies from the parent population are shown. SSC, side scatter. (d) Single-cell clustering of individual cord blood pre-cDCs (three samples). This analysis shows that cord blood pre-cDCs cluster in CD1c$^+$ lineage–primed (266 single cells; blue), CD141$^+$ lineage–primed (29 single cells; red), and non-DCs (157 single cells; gray). Shown are the top 30 genes exhibiting the strongest differential expression for each lineage-primed subset ($P < 10^{-5}$; likelihood ratio test for single-cell differential expression; see the Single-cell mRNA sequencing section of Materials and methods and Table S2). (e) Expression of selected genes in CD1c$^+$ lineage–primed cells (blue), CD141$^+$ lineage–primed cells (red), and non-DCs (gray) presented as violin plots (y axis, gene expression; x-axis, abundance of cells expressing the gene).

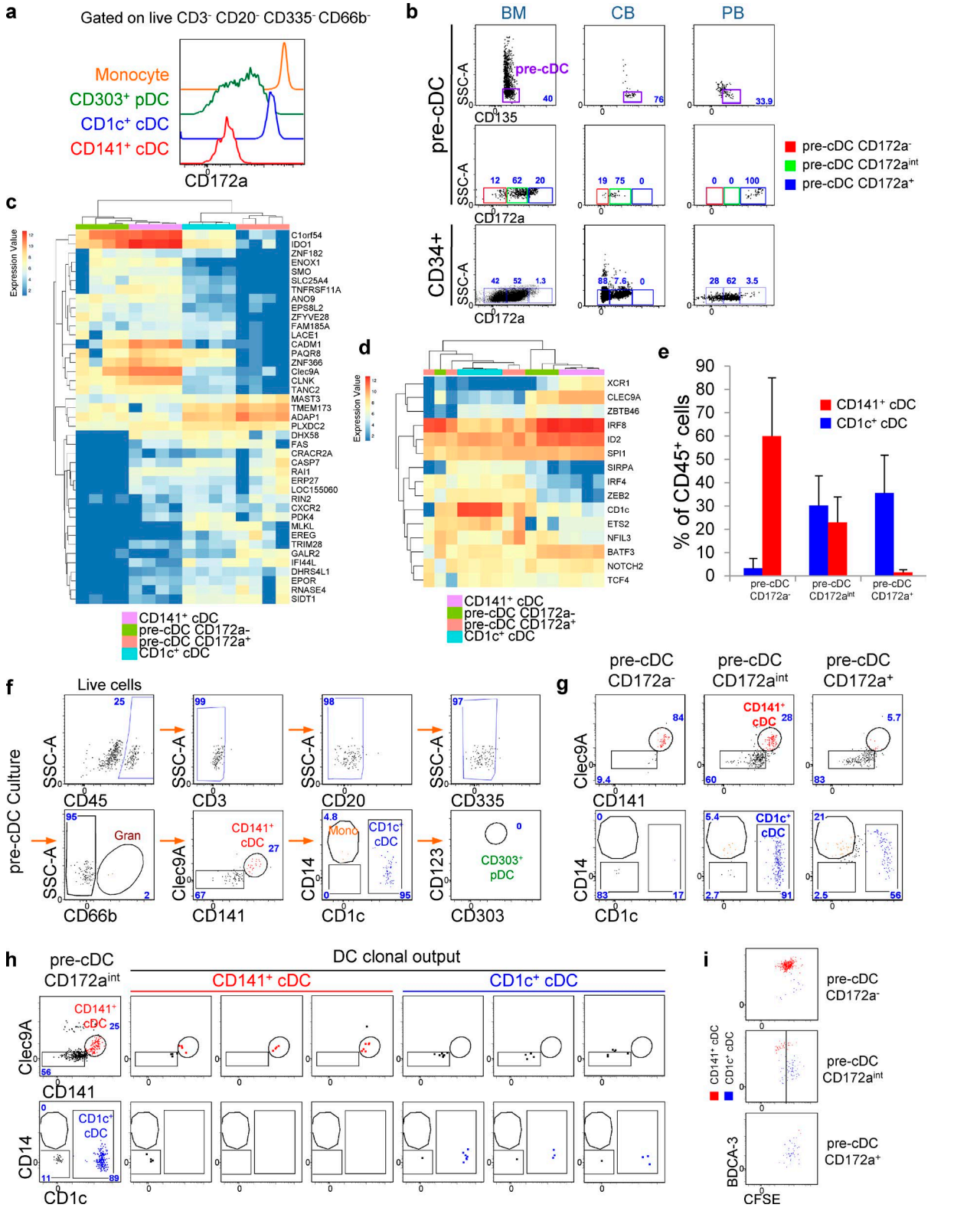

Figure 2. **Heterogeneous expression of CD172a in human cord blood pre-cDCs identifies populations with CD1c⁺ or CD141⁺ lineage potential.** (a) Expression of CD172a receptor on cDCs and monocytes. The flow cytometry histogram shows expression of CD172a on live CD3⁻ CD20⁻ CD335⁻ CD66b⁻–gated monocytes (CD14⁺; orange), pDCs (CD303⁺; green), CD1c⁺ cDCs (blue), and CD141⁺ cDCs (red) from peripheral blood ($n = 3$). (b) Expression of CD172a receptor on pre-cDCs in human cord blood (CB), bone marrow, and peripheral blood (PB; cord blood, $n = 6$; bone marrow, $n = 2$; peripheral blood, $n = 3$). Flow

Peripheral blood pre-cDCs differed from their cord blood counterparts by showing a more mature phenotype. All subpopulations expressed higher levels of HLA-DR, CD11c, and their respective lineage-restricted transcription factors, i.e., IRF8 and IRF4 (Fig. 3 c). Interestingly, the non-DCs found in peripheral blood lost CSF-R and express some of the same markers as the $CD1c^+$ lineage–primed subpopulation including IRF4, HLA-DR, and CD11c. Thus, this subgroup may represent precursors of the $CD1c^+$ lineage in circulation and therefore differ from the cord blood non-DCs.

Flt3L injection induces mobilization of human pre-cDC subsets

To examine the regulation of the two pre-cDC subsets in humans, we assayed the blood from three volunteers who received 25 µg/kg Flt3L subcutaneously on seven consecutive days. Mature $CD1c^+$ and $CD141^+$ cDCs increase proportionally in the blood in response to Flt3L injection (Pulendran et al., 2000; Breton et al., 2015b) as do pre-cDCs (Fig. 4, a and b). Both pre-cDC subsets were mobilized by Flt3L. However, in two out of the three subjects tested, circulating $CD172a^+$ pre-cDCs are far more responsive to Flt3L than $CD172a^-$ pre-cDCs, which also express lower levels of HLA-DR and higher levels of CD117 than $CD172a^+$ pre-cDCs, suggesting that the later are less mature and retained in the bone marrow (Fig. 4 c).

In summary, we have defined circulating precursors that are committed to the $CD1c^+$ and $CD141^+$ cDC lineages in humans. These progenitors express nonoverlapping sets of cDC subset–specific transcription factors, and they show in vivo expansion after Flt3L injection.

MATERIALS AND METHODS

Human cell samples

Human umbilical cord blood was purchased from the New York Blood Center. Human bone marrow was obtained from total hip arthroplasty at the Hospital for Special Surgery (New York, NY). Peripheral Blood was obtained from The Rockefeller University Hospital (New York, NY). All studies were approved by the Institutional Review Board of The Rockefeller University Hospital. Individual participants in these studies provided written informed consent. Fresh cord blood and PBMCs were isolated by density centrifugation using Ficoll-Hypaque. Bone marrow mononuclear cells were isolated by density centrifugation using Ficoll-Hypaque after digestion with collagenase IV. Aliquots of mononuclear bone marrow cells were frozen and stored in liquid nitrogen for future analysis. Samples from cord blood, peripheral blood, and bone marrow were incubated with fluorescence-labeled antibodies for direct analysis on a flow cytometer (LSRII; BD) or further purification by fluorescence-activated cell sorting on a cell sorter (FACSAria III; BD). For a more detailed protocol, see Breton et al. (2015a).

pre-cDC isolation and in vitro differentiation

After density centrifugation using Ficoll-Hypaque, cord blood mononuclear cells were stained using CD3, CD20, CD14, CD66b, CD335, CD10, CD303, CD1c, CD141, CD123, CD34, CD117, CD116, CD135, CD115, CD45RA, and CD172a antibodies. Three subpopulations of pre-cDCs were isolated as Lin (CD3/20/14/66b/335/10)$^-$ DC (CD303/CD1c/CD141)$^-$ $CD34^-$ $CD117^+$ $CD123^{-/+}$ $CD135^+$ $CD116^+$ $CD115^-$ $CD45RA^+$ and $CD172a^-$, $CD172a^+$, or $CD172a^{int}$. These progenitor cells were then cultured on MS-5 stromal cells plus cytokines Flt3L, SCF, and GM-CSF. Cells were harvested at day 7 for flow cytometry analysis of the culture output. Cultured cells were stained with Live/Dead, CD45, CD3, CD20, CD14, CD66b, CD335, CD303, CD123, CD1c, CD141, and Clec9A antibodies for 30 min on ice. Cells were fixed with 2% formaldehyde and stored at 4°C until analysis, which was performed on a flow cytometer (LSRII; BD). Analysis was performed using Flow Jo software (9.1; Tree Star). For single-cell clonal assay, individual pre-cDCs were sorted into each well containing mitomycin

cytometry plots show that Lin^- $CD34^-$ $CD117^+$ $CD123^{-/+}$ $CD135^+$ $CD115^-$ $CD116^+$ pre-cDCs in human cord blood can be divided by CD172a into three populations: $CD172a^-$ (red), $CD172a^{int}$ (green), and $CD172a^+$ (blue) pre-cDCs. Gate frequencies from parent population are shown. SSC, side scatter. (c) Heat map showing the top 41 differentially expressed genes selected by unsupervised hierarchical clustering (clustering analysis on all differentially expressed genes with p-value <0.05) between cord blood $CD172a^+$ ($n = 4$), cord blood $CD172a^-$ pre-cDCs ($n = 4$), peripheral blood $CD141^+$ cDCs ($n = 4$), and peripheral blood $CD1c^+$ cDCs ($n = 4$; Table S3). (d) Expression of specific surface markers and lineage-restricted transcription factors involved in DC development in $CD1c^+$ cDCs, $CD141^+$ cDCs, $CD172a^+$ pre-cDCs, and $CD172a^-$ pre-cDCs. (e) The graph shows mean output of $CD141^+$ cDCs (red) and $CD1c^+$ cDCs (blue) from the culture of $CD172a^-$, $CD172a^{int}$, and $CD172a^+$ pre-cDCs from five independent experiments. Error bars represent the standard deviation. (f) Gating strategy for culture output after hematopoietic differentiation on MS-5 stromal cells of human cord blood pre-cDCs. Total cord blood pre-cDCs were isolated and then cultured in MS5 + FSG for 7 d. Culture output was assessed by flow cytometry. Cells developing into culture are identified within the live Lin^- $CD45^+$ cells. Output cells include $CD66b^+$ granulocytes (Gran; brown), $CD141^+$ cDCs (red), $CD1c^+$ cDCs (blue), monocytes (Mono; orange), and $CD303^+$ pDCs (green). Gate frequencies from the parent population are shown ($n = 5$). (g) Differentiation potential of 50–200 purified cells from cord blood $CD172a^-$, $CD172a^{int}$, and $CD172a^+$ pre-cDCs in MS5 + FSG cultures for 7 d. Flow cytometry plots show gated Lin^- $CD45^+$ cells. $CD141^+$ cDCs were identified as $CD141^+$ $CLEC9A^+$ and $CD1c^+$ cDCs as $CLEC9A^-$ $CD14^-$ $CD1c^+$ ($n = 5$). Gate frequencies from the parent population are shown. (h) Single-cell clonal assay of $CD172a^{int}$ pre-cDCs. Representative flow cytometry of gated Lin^- $CD45^+$ cells derived from single $CD172a^{int}$ pre-cDC culture show clonal output of $CD141^+$ cDCs (red) and $CD1c^+$ cDCs (blue). For this representative experiment, 11 wells gave rise to $CD141^+$ cDCs and 33 wells to $CD1c^+$ cDCs (120 wells plated; 44 positive wells; $n = 3$). (i) Proliferative capacity of $CD172a^-$, $CD172a^{int}$, and $CD172a^+$ pre-cDCs. pre-cDC subsets were purified from cord blood, labeled with CFSE, and cultured in MS5 + FSG for 7 d. Proliferation was assessed by flow cytometry. Representative FACS plots show $CD141^+$ cDCs (red) and $CD1c^+$ cDCs (blue) CFSE dilution ($n = 2$).

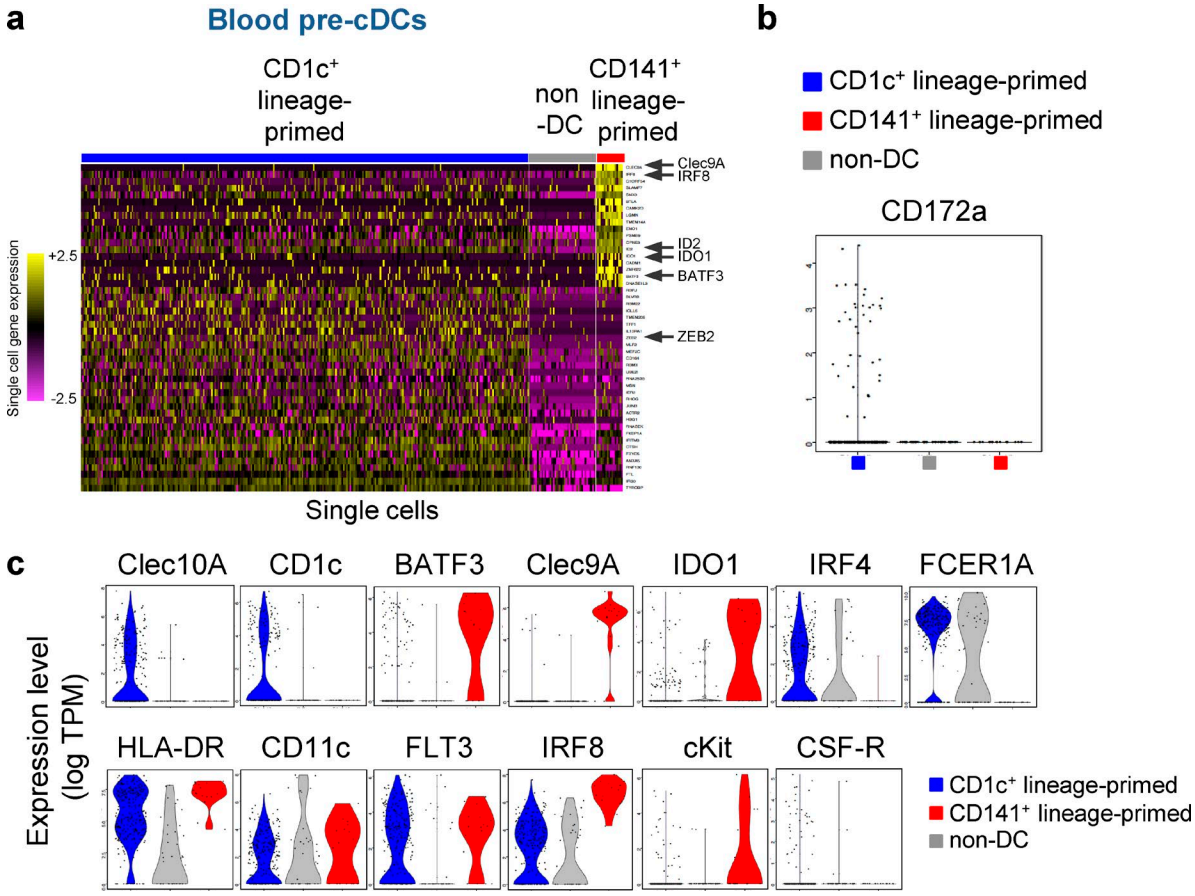

Figure 3. **Human blood subsets of pre-cDCs.** (a) Single-cell clustering for individual peripheral blood pre-cDCs. This analysis showed that peripheral blood pre-cDCs cluster in CD1c$^+$ lineage–primed (282 single cells; blue), CD141$^+$ lineage–primed (17 single cells; red), and non-DC (42 single cells; gray) populations (three samples). Shown are the top 30 genes exhibiting the strongest differential expression for each lineage-primed subset ($P < 10^{-5}$; likelihood ratio test for single-cell differential expression; see the Single-cell mRNA sequencing section of Materials and methods and Table S4). (b and c) Expression of CD172a (b) and selected genes (c) in CD1c$^+$ lineage–primed cells (blue), CD141$^+$ lineage–primed cells (red), and non-DCs (gray) presented as violin plots (y axis, gene expression; x axis, abundance of cells expressing the gene).

C–pretreated MS-5 stromal cells and Flt3L, SCF, and GM-CSF. After 7 d of culture, each well was analyzed for culture output by flow cytometry. For a more detailed protocol, see Breton et al. (2015a).

CFSE labeling

CFSE (Molecular Probes) was resuspended in DMSO at a concentration of 5 mM and stored at −80°C. Each batch of CFSE was titrated beforehand on PBMCs to determine optimal concentration for labeling (0.5 µM in our study). PBMCs were washed twice in PBS and resuspended in PBS at a 2 × 10^7 cells per milliliter concentration. A 1-µM working solution of CFSE was prepared from the stock by dilution in PBS. For labeling, one volume of working solution of CFSE was added to one volume of PBMCs. The cells were incubated in the dark with gentle mixing at room temperature for 8 min. The reaction was quenched by addition of an equal volume of human serum for 2 min. Cells were washed twice with PBS and resuspended in RPMI 10% human serum. For CFSE assays, cultured cells were stained with Live/Dead, CD45, CD3, CD20, CD14, CD66b, CD335, CD303, CD123, CD1c, CD141, and Clec9A antibodies for 30 min on ice. For a more detailed protocol, see Breton et al. (2015a).

RNA isolation and mRNA sequencing

RNA from sorted cord blood pre-cDC subsets (150–400 cells) and peripheral blood cDC subsets (2,000–10,000 cells) pellets was extracted and column purified using a PicoPure RNA Isolation kit (Arcturus; Applied Biosystems). Genomic DNA was removed by on-column digest with DNase I (QIAGEN), according to the PicoPure RNA Isolation kit manual. RNA libraries were prepared using the SMARTer Ultra Low Input RNA for Sequencing kit (Takara Bio Inc.) followed by preparation with a DNA Library Prep kit (Nextera XT; Illumina). Libraries were sequenced by 75-bp single-end reading on a NextSeq 500 sequencer (Illumina).

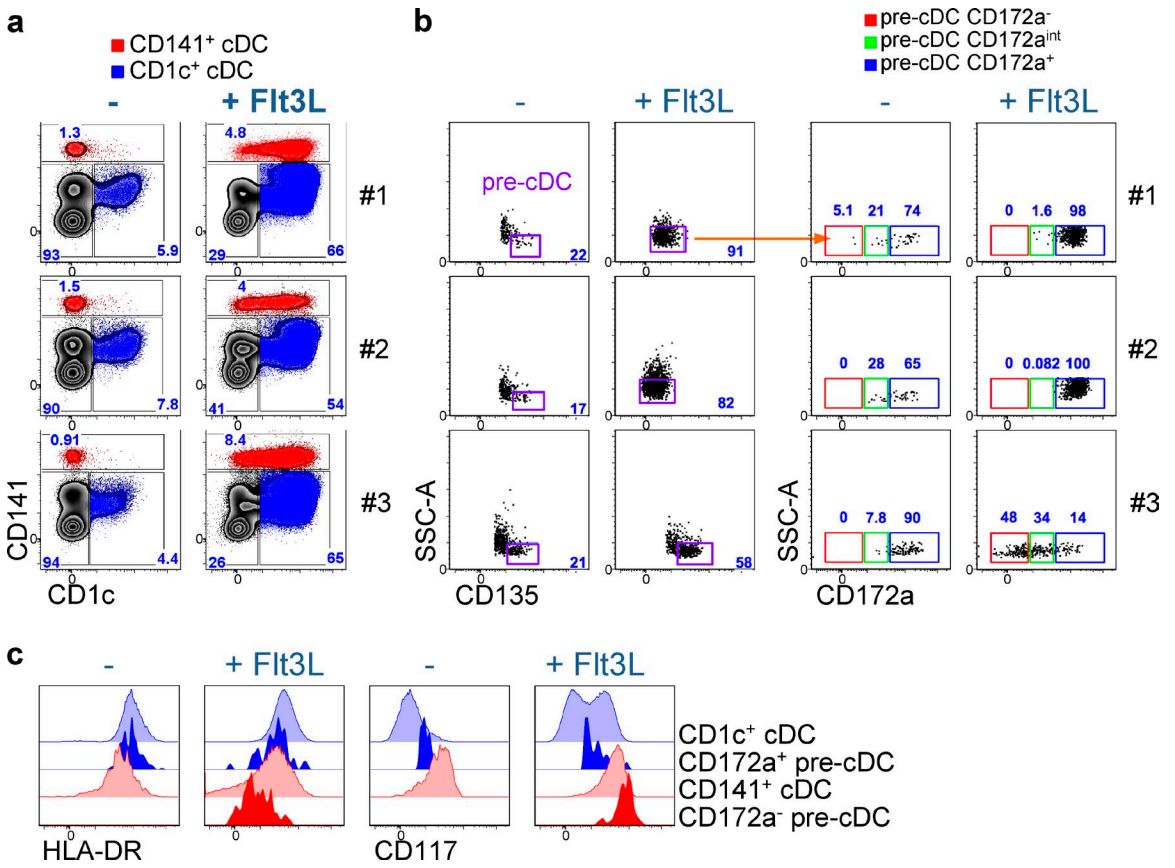

Figure 4. **Flt3L mobilizes human CD172a⁻ and CD172a⁺ pre-cDCs into the blood.** (a and b) PBMCs from Flt3L-injected volunteers (n = 3; 25 µg/kg for seven consecutive days) were analyzed by flow cytometry before (day 0) and after Flt3L treatment (day 12) to assess the expansion of CD1c⁺ and CD141⁺ cDC subsets as well as CD172a⁻, CD172a^{int}, and CD172a⁺ pre-cDC subsets in blood. Representative flow cytometry dot plots show CD1c⁺ cDCs (blue) and CD141⁺ cDCs (red; a) as well as CD172a⁻ (red), CD172a^{int} (green), and CD172a⁺ (blue; b) pre-cDC subsets (gating strategy in Fig. 1, a and c). Gate frequencies from parent population are shown. SSC, side scatter. (c) Representative histogram shows CD117 and HLA-DR expression on CD1c⁺ cDCs, CD141⁺ cDCs, CD172a⁻ pre-cDCs, and CD172a⁺ pre-cDCs in one of the Flt3L-treated volunteers.

The reads were aligned using STAR software (version 2.3.0) that permits unique alignments to human genes (GRCh37/hg19; Dobin et al., 2013). HTSeq was used to generate a gene expression counts table from STAR output (Anders et al., 2015). The normalization, dispersion estimation, and test for differential expression were done with DESeq2 (v1.10.1; Love et al., 2014). The unsupervised hierarchical clustering and heat maps plots were generated with the pvclust R package (Suzuki and Shimodaira, 2006). Data are available in the National Center for Biotechnology Information GEO DataSets under accession no. GSE88858.

Single-cell mRNA sequencing

Single-cell RNA-seq analyses. Single-cell libraries were prepared using the SMART-Seq 2 protocol (Picelli et al., 2013). In brief, single cells were sorted into single wells of a 96-well plate, where wells were preloaded with reverse transcription buffer and primer and processed as previously described (Efroni et al., 2016).

Raw data processing. Raw sequencing data were processed as previously described (Shalek et al., 2014). In brief, short sequencing reads were aligned to the University of California, Santa Cruz (UCSC) hg19 transcriptome and were also used as input in RSEM (v 1.2.1) to quantify gene expression levels (transcripts per million [TPM]) for all UCSC hg19 genes in all samples. We filtered out cells from our dataset where we detected <1,000 unique genes per cell. All genes that were not detected in at least 1% of all our single cells were discarded, leaving 20,869 genes for all further analyses. Data were log transformed (logTPM + 1) for all downstream analyses.

Identifying markers of cell type. Sorted CD1c⁺ and CD141⁺ cDCs profiled by single-cell mRNA sequencing were easily distinguished by the expression of known markers. To identify an unbiased gene set distinguishing CD1c⁺ versus CD141⁺ cDCs of individual single-cell clusters, we implemented a likelihood ratio test for single-cell differential expression (McDavid et al., 2013). Importantly, this test is designed to

simultaneously test for changes in both the percentage of cells expressing a gene as well as the quantitative RNA levels with these cells. We identified 321 genes that were differentially expressed at P < 1e-2 (Bonferroni correction) and 122 genes that were differentially expressed at P < 1e-5 (Bonferroni correction).

Identifying lineage-primed states in single-cell RNA-seq data. We clustered single-cell RNA-seq data from pre-cDCs using the Seurat package (Macosko et al., 2015; Satija et al., 2015). We followed the same procedure for both cord blood and peripheral blood pre-cDC experiments. First, we identified a set of variable genes across all cells by searching for genes with high variance after controlling for their average expression across all cells, as described by Satija et al. (2015). We supplemented this gene set with the set of 122 highly significant genes that distinguished $CD1c^+$ versus $CD141^+$ as described in the previous paragraph. Next, we perform a principal component (PC) analysis to reduce the dimensionality of our data using this input gene set. Then, we performed a permutation test to identify a set of statistically significant components, whose gene loadings were greater than observed in randomly permuted datasets (Satija et al., 2015), verified that our selected PCs fell before the knee of the commonly used scree plot, and removed PCs that were primarily defined by ribosomal or mitochondrial genes, which have been shown to be markers of technical variation in single-cell RNA-seq (Ilicic et al., 2016). Finally, we partitioned single cells based on this reduced dimensional space using k-means clustering.

Next, we identified markers of each identified cluster using the same likelihood ratio test described in the previous paragraph. We tested all 20,869 genes in this process and, for each cluster, identified gene sets that were positively enriched (P < 1e-2; Bonferroni correction) in members of the cluster, compared with all other cells.

We observed that cluster markers in the pre-cDCs included many canonical markers of $CD1c^+$ and $CD141^+$ DCs. To test the statistical significance of the overlap between the marker sets, we used a Fisher's exact test, as implemented in the GeneOverlap package in R. In both the cord blood and peripheral blood datasets, we observed pre-cDC cell subsets whose markers were strongly overlapping with both $CD1c^+$ and $CD141^+$ DCs and therefore refer to these cells as lineage-primed cells.

Data are available in the National Center for Biotechnology Information GEO DataSets under accession no. GSE89232.

Flt3L injection in volunteers

Three healthy volunteers received a 25-µg/kg/day injection of CDX-301 (a clinical formulation of recombinant human Flt3L; Celldex) for seven consecutive days. This phase 1 study was done at The Rockefeller University Hospital by N. Anandasabapathy, S. Schlesinger, and M. Caskey (The Rockefeller University, New York, NY). Blood samples were collected before (day 0) and after (day 12) initial treatment. PBMCs were isolated from heparinized blood using Ficoll-Hypaque and stored in liquid nitrogen for further analysis. Cells were stained with CD3, CD20, CD14, CD66b, CD335, CD10, CD303, CD1c, CD141, CD123, CD34, CD117, CD116, CD135, CD115, CD45RA, and CD172a antibodies. Cells were fixed with 2% formaldehyde and stored at 4°C until analysis, which was performed on a flow cytometer (LSRII; BD). Analysis was performed using Flow Jo software (9.1; Tree Star). For a more detailed protocol, see Breton et al. (2015a,b).

Online supplemental material

Tables S1–S4 are included as Excel files. Table S1 shows the genes (321) exhibiting the strongest differential expression for single differentiated blood $CD1c^+$ cDCs (n = 77) and $CD141^+$ cDCs (n = 87; P < 10^{-5}; likelihood ratio test for single-cell differential expression). Table S2 lists the genes (298) exhibiting the strongest differential expression for each cord blood lineage–primed subset of pre-cDCs, i.e., $CD1c^+$ lineage primed (266 clones), $CD141^+$ lineage primed (29 clones), and non-DCs (157 clones; P < 10^{-5}; likelihood ratio test for single-cell differential expression). Table S3 shows the top 41 genes differentially expressed for bulk $CD1c^+$ cDCs (n = 4), $CD141^+$ cDCs (n = 4), $CD172a^-$ pre-cDCs (n = 4), and $CD172a^+$ pre-cDCs (n = 4; P-value <0.05). Table S4 lists the genes (104) exhibiting the strongest differential expression for each blood lineage–primed subset of pre-cDCs, i.e., $CD1c^+$ lineage–primed (282 clones), $CD141^+$ lineage–primed (17 clones), and non-DC populations (42 clones; P < 10^{-5}; likelihood ratio test for single-cell differential expression).

ACKNOWLEDGMENTS

We thank Klara Velinzon (Flow Cytometry Core Facility, Laboratory of Molecular Immunology, The Rockefeller University, New York, NY) for technical support with polychromatic flow cytometry sorting. We thank Niroshana Anandasabapathy, Sarah Schlesinger, and Marina Caskey for the Flt3L patient samples. We thank Arlene Hurley and the clinical team at the Rockefeller University Hospital.

Research reported in this publication was supported by a National Institutes of Health National Center for Advancing Translational Sciences grant (UL1TR0000-43-10) to G. Breton, a National Institutes of Health grant (DP2-HG-009623) to R. Satija, and a National Institutes of Health grant (1U19AI111825-01) to M.C. Nussenzweig. M.C. Nussenzweig is a Howard Hughes Medical Institute investigator.

The authors declare no competing financial interests.

Submitted: 19 July 2016
Revised: 6 October 2016
Accepted: 21 October 2016

REFERENCES

Anders, S., P.T. Pyl, and W. Huber. 2015. HTSeq—a Python framework to work with high-throughput sequencing data. *Bioinformatics.* 31:166–169. http://dx.doi.org/10.1093/bioinformatics/btu638

Bachem, A., S. Güttler, E. Hartung, F. Ebstein, M. Schaefer, A. Tannert, A. Salama, K. Movassaghi, C. Opitz, H.W. Mages, et al. 2010. Superior antigen cross-presentation and XCR1 expression define human $CD11c^+CD141^+$ cells as homologues of mouse $CD8^+$ dendritic cells. *J. Exp. Med.* 207:1273–1281. http://dx.doi.org/10.1084/jem.20100348

Breton, G., J. Lee, K. Liu, and M.C. Nussenzweig. 2015a. Defining human dendritic cell progenitors by multiparametric flow cytometry. *Nat. Protoc.* 10:1407–1422. http://dx.doi.org/10.1038/nprot.2015.092

Breton, G., J. Lee, Y.J. Zhou, J.J. Schreiber, T. Keler, S. Puhr, N. Anandasabapathy, S. Schlesinger, M. Caskey, K. Liu, and M.C. Nussenzweig. 2015b. Circulating precursors of human CD1c$^+$ and CD141$^+$ dendritic cells. *J. Exp. Med.* 212:401–413. http://dx.doi.org/10.1084/jem.20141441

Cohn, L., B. Chatterjee, F. Esselborn, A. Smed-Sörensen, N. Nakamura, C. Chalouni, B.C. Lee, R. Vandlen, T. Keler, P. Lauer, et al. 2013. Antigen delivery to early endosomes eliminates the superiority of human blood BDCA3$^+$ dendritic cells at cross presentation. *J. Exp. Med.* 210:1049–1063. http://dx.doi.org/10.1084/jem.20121251

Colonna, M., G. Trinchieri, and Y.J. Liu. 2004. Plasmacytoid dendritic cells in immunity. *Nat. Immunol.* 5:1219–1226. http://dx.doi.org/10.1038/ni1141

Crozat, K., R. Guiton, V. Contreras, V. Feuillet, C.A. Dutertre, E. Ventre, T.P. Vu Manh, T. Baranek, A.K. Storset, J. Marvel, et al. 2010. The XC chemokine receptor 1 is a conserved selective marker of mammalian cells homologous to mouse CD8α$^+$ dendritic cells. *J. Exp. Med.* 207:1283–1292. http://dx.doi.org/10.1084/jem.20100223

Dobin, A., C.A. Davis, F. Schlesinger, J. Drenkow, C. Zaleski, S. Jha, P. Batut, M. Chaisson, and T.R. Gingeras. 2013. STAR: ultrafast universal RNA-seq aligner. *Bioinformatics.* 29:15–21. http://dx.doi.org/10.1093/bioinformatics/bts635

Efroni, I., A. Mello, T. Nawy, P.L. Ip, R. Rahni, N. DelRose, A. Powers, R. Satija, and K.D. Birnbaum. 2016. Root regeneration triggers an embryo-like sequence guided by hormonal interactions. *Cell.* 165:1721–1733. http://dx.doi.org/10.1016/j.cell.2016.04.046

Grajales-Reyes, G.E., A. Iwata, J. Albring, X. Wu, R. Tussiwand, W. Kc, N.M. Kretzer, C.G. Briseño, V. Durai, P. Bagadia, et al. 2015. Batf3 maintains autoactivation of *Irf8* for commitment of a CD8α$^+$ conventional DC clonogenic progenitor. *Nat. Immunol.* 16:708–717. http://dx.doi.org/10.1038/ni.3197

Ilicic, T., J.K. Kim, A.A. Kolodziejczyk, F.O. Bagger, D.J. McCarthy, J.C. Marioni, and S.A. Teichmann. 2016. Classification of low quality cells from single-cell RNA-seq data. *Genome Biol.* 17:29. http://dx.doi.org/10.1186/s13059-016-0888-1

Jin, J.O., W. Zhang, J.Y. Du, and Q.Yu. 2014. BDCA1-positive dendritic cells (DCs) represent a unique human myeloid DC subset that induces innate and adaptive immune responses to *Staphylococcus aureus* infection. *Infect. Immun.* 82:4466–4476. http://dx.doi.org/10.1128/IAI.01851-14

Jongbloed, S.L., A.J. Kassianos, K.J. McDonald, G.J. Clark, X. Ju, C.E. Angel, C.J. Chen, P.R. Dunbar, R.B. Wadley, V. Jeet, et al. 2010. Human CD141$^+$ (BDCA-3)$^+$ dendritic cells (DCs) represent a unique myeloid DC subset that cross-presents necrotic cell antigens. *J. Exp. Med.* 207:1247–1260. http://dx.doi.org/10.1084/jem.20092140

Lee, J., G. Breton, T.Y. Oliveira, Y.J. Zhou, A. Aljoufi, S. Puhr, M.J. Cameron, R.P. Sékaly, M.C. Nussenzweig, and K. Liu. 2015. Restricted dendritic cell and monocyte progenitors in human cord blood and bone marrow. *J. Exp. Med.* 212:385–399. http://dx.doi.org/10.1084/jem.20141442

Love, M.I., W. Huber, and S. Anders. 2014. Moderated estimation of fold change and dispersion for RNA-seq data with DESeq2. *Genome Biol.* 15:550. http://dx.doi.org/10.1186/s13059-014-0550-8

Macosko, E.Z., A. Basu, R. Satija, J. Nemesh, K. Shekhar, M. Goldman, I. Tirosh, A.R. Bialas, N. Kamitaki, E.M. Martersteck, et al. 2015. Highly parallel genome-wide expression profiling of individual cells using nanoliter droplets. *Cell.* 161:1202–1214. http://dx.doi.org/10.1016/j.cell.2015.05.002

Manicassamy, S., and B. Pulendran. 2011. Dendritic cell control of tolerogenic responses. *Immunol. Rev.* 241:206–227. http://dx.doi.org/10.1111/j.1600-065X.2011.01015.x

McDavid, A., G. Finak, P.K. Chattopadyay, M. Dominguez, L. Lamoreaux, S.S. Ma, M. Roederer, and R. Gottardo. 2013. Data exploration, quality control and testing in single-cell qPCR-based gene expression experiments. *Bioinformatics.* 29:461–467. http://dx.doi.org/10.1093/bioinformatics/bts714

Notta, F., S. Zandi, N. Takayama, S. Dobson, O.I. Gan, G. Wilson, K.B. Kaufmann, J. McLeod, E. Laurenti, C.F. Dunant, et al. 2016. Distinct routes of lineage development reshape the human blood hierarchy across ontogeny. *Science.* 351:aab2116. http://dx.doi.org/10.1126/science.aab2116

Paul, F., Y. Arkin, A. Giladi, D.A. Jaitin, E. Kenigsberg, H. Keren-Shaul, D. Winter, D. Lara-Astiaso, M. Gury, A. Weiner, et al. 2015. Transcriptional heterogeneity and lineage commitment in myeloid progenitors. *Cell.* 163:1663–1677. http://dx.doi.org/10.1016/j.cell.2015.11.013

Perié, L., K.R. Duffy, L. Kok, R.J. de Boer, and T.N. Schumacher. 2015. The branching point in erythro-myeloid differentiation. *Cell.* 163:1655–1662. http://dx.doi.org/10.1016/j.cell.2015.11.059

Persson, E.K., H. Uronen-Hansson, M. Semmrich, A. Rivollier, K. Hägerbrand, J. Marsal, S. Gudjonsson, U. Håkansson, B. Reizis, K. Kotarsky, and W.W. Agace. 2013. IRF4 transcription-factor-dependent CD103$^+$CD11b$^+$ dendritic cells drive mucosal T helper 17 cell differentiation. *Immunity.* 38:958–969. http://dx.doi.org/10.1016/j.immuni.2013.03.009

Picelli, S., A.K. Björklund, O.R. Faridani, S. Sagasser, G. Winberg, and R. Sandberg. 2013. Smart-seq2 for sensitive full-length transcriptome profiling in single cells. *Nat. Methods.* 10:1096–1098. http://dx.doi.org/10.1038/nmeth.2639

Poulin, L.F., M. Salio, E. Griessinger, F. Anjos-Afonso, L. Craciun, J.L. Chen, A.M. Keller, O. Joffre, S. Zelenay, E. Nye, et al. 2010. Characterization of human DNGR-1$^+$ BDCA3$^+$ leukocytes as putative equivalents of mouse CD8α$^+$ dendritic cells. *J. Exp. Med.* 207:1261–1271. http://dx.doi.org/10.1084/jem.20092618

Pulendran, B., J. Banchereau, S. Burkeholder, E. Kraus, E. Guinet, C. Chalouni, D. Caron, C. Maliszewski, J. Davoust, J. Fay, and K. Palucka. 2000. Flt3-ligand and granulocyte colony-stimulating factor mobilize distinct human dendritic cell subsets in vivo. *J. Immunol.* 165:566–572. http://dx.doi.org/10.4049/jimmunol.165.1.566

Robbins, S.H., T. Walzer, D. Dembélé, C. Thibault, A. Defays, G. Bessou, H. Xu, E. Vivier, M. Sellars, P. Pierre, et al. 2008. Novel insights into the relationships between dendritic cell subsets in human and mouse revealed by genome-wide expression profiling. *Genome Biol.* 9:R17. http://dx.doi.org/10.1186/gb-2008-9-1-r17

Satija, R., J.A. Farrell, D. Gennert, A.F. Schier, and A. Regev. 2015. Spatial reconstruction of single-cell gene expression data. *Nat. Biotechnol.* 33:495–502. http://dx.doi.org/10.1038/nbt.3192

Schlitzer, A., N. McGovern, P. Teo, T. Zelante, K. Atarashi, D. Low, A.W. Ho, P. See, A. Shin, P.S. Wasan, et al. 2013. IRF4 transcription factor-dependent CD11b$^+$ dendritic cells in human and mouse control mucosal IL-17 cytokine responses. *Immunity.* 38:970–983. http://dx.doi.org/10.1016/j.immuni.2013.04.011

Schlitzer, A., V. Sivakamasundari, J. Chen, H.R. Sumatoh, J. Schreuder, J. Lum, B. Malleret, S. Zhang, A. Larbi, F. Zolezzi, et al. 2015. Identification of cDC1- and cDC2-committed DC progenitors reveals early lineage priming at the common DC progenitor stage in the bone marrow. *Nat. Immunol.* 16:718–728. http://dx.doi.org/10.1038/ni.3200

Shalek, A.K., R. Satija, J. Shuga, J.J. Trombetta, D. Gennert, D. Lu, P. Chen, R.S. Gertner, J.T. Gaublomme, N. Yosef, et al. 2014. Single-cell RNA-seq reveals dynamic paracrine control of cellular variation. *Nature.* 510:363–369.

Steinman, R.M., and J. Banchereau. 2007. Taking dendritic cells into medicine. *Nature.* 449:419–426. http://dx.doi.org/10.1038/nature06175

Steinman, R.M., and H. Hemmi. 2006. Dendritic cells: translating innate to adaptive immunity. *In* Innate Immunity to Immunological Memory. B. Pulendran and R. Ahmed, editors. Springer-Verlig, Berlin, Heidelberg. 17–58. http://dx.doi.org/10.1007/3-540-32636-7_2

Suzuki, R., and H. Shimodaira. 2006. Pvclust: an R package for assessing the uncertainty in hierarchical clustering. *Bioinformatics.* 22:1540–1542. http://dx.doi.org/10.1093/bioinformatics/btl117

Villadangos, J.A., and K. Shortman. 2010. Found in translation: the human equivalent of mouse $CD8^+$ dendritic cells. *J. Exp. Med*. 207:1131–1134. http://dx.doi.org/10.1084/jem.20100985